2006

# Probabilistic Determination of Two-Phase Flow Regimes Utilizing an Automated Image Recognition Technique

Emad W. Jassim
*University of Illinois at Urbana-Champaign*

Ty A. Newell
*University of Illinois at Urbana-Champaign*

John C. Chato
*University of Illinois at Urbana-Champaign*

# Probabilistic Determination of Two-Phase Flow Regimes Utilizing an Automated Image Recognition Technique

Emad W. Jassim[1]*, Ty A. Newell[2], and John C. Chato[3]

[1]University of Illinois, Department of Mechanical and Industrial Engineering
Urbana, IL, USA
Tel: 217-377-8249, Fax: 217-333-1942, E-mail: jassim@uiuc.edu

[2]University of Illinois, Department of Mechanical and Industrial Engineering
Urbana, IL, USA
Tel: 217-333-2280, Fax: 217-244-6534, E-mail: tynewell@uiuc.edu

[3]University of Illinois, Department of Mechanical and Industrial Engineering
Urbana, IL, USA
Tel: 217-244-9853, Fax: 217-244-6534, E-mail: jbchato@uiuc.edu

*Corresponding Author

## ABSTRACT

Probabilistic two-phase flow map models are used in the literature to predict pressure drop and void fraction in multi-port microchannels. In the present study probabilistic two-phase flow maps are experimentally developed for R134a at 25, 35, and 50$^{o}$C, R410A at 25$^{o}$C, mass fluxes from 100 to 600kg/m$^{2}$-s, qualities from 0 to1 in 8mm, 5.4mm, 3.9mm, 1.7mm I.D. smooth adiabatic tubes in order to extend the probabilistic two-phase flow map modeling technique to single tubes. A new web camera based flow visualization technique utilizing an illuminated diffuse stripped background was utilized to enhance images, detect fine films, and aid in the automated image recognition process. The developed automated image recognition software determines the flow regime time fraction in approximately 900 images per flow condition (~1 million images total). The maximum and average error in the automated flow regime time fraction determination is found to be 4% and 0.6% respectively.

## 1. INTRODUCTION

Flow regime maps developed from flow visualization observations are commonly used or developed in the literature such as Wojtan et al. (2005a&b)), Garimella (2004), Garimella et al. (2003), Coleman and Garimella et al. (2003), El Hajal et al. (2003), Thome et al. (2003), Didi et al. (2002), Zurcher et al. (2002a&b), Dobson and Chato (1998), Mandhane et al. (1974), and Baker (1954) to aid in the modeling of two-phase flow. The three main types of two-phase flow regime maps in the literature Baker/Mandhane, Taitel-Dukler, and the most commonly used Steiner type depict boundaries between flow regimes that are not easily represented by continuous functions. This is evident from figure 1, which contains a typical Steiner type flow map that has recently been developed by Wojtan et al. (2005a) and used to predict heat transfer coefficients by Wojtan et al. (2005b). Two phase flow models that incorporate these traditional flow maps are complicated in order to eliminate discontinuities at flow regime boundaries and incorporate the flow regime information as functions. Furthermore, Jassim and Newell (2006), Coleman and Garimella (2003), El Hajal et al. (2003), and Niño (2002) indicate that more than one flow regime can exist near the boundaries or within a given flow regime on a Steiner type flow map.

Probabilistic two-phase flow regime maps first developed by Niño (2002) for refrigerant and air-water flow in multi-port microchannels are found by Jassim and Newell (2006) to eliminate the discontinuities created by traditional flow maps. Probabilistic two phase flow regime maps have quality on the horizontal axis and the fraction of time in which a particular flow regime is observed in a series of pictures taken at given flow condition (F) on the y axis as seen in figure 2. Jassim and Newell (2006) developed curve fit functions to represent the data that are continuous for the entire quality range with correct physical limits for the time fraction data obtained for 6-port microchannels by Niño (2002). Jassim and Newell (2006) then utilized the probabilistic flow regime map time fraction curve fits to predict pressure drop and void fraction as shown in equations 1 and 2 respectively.

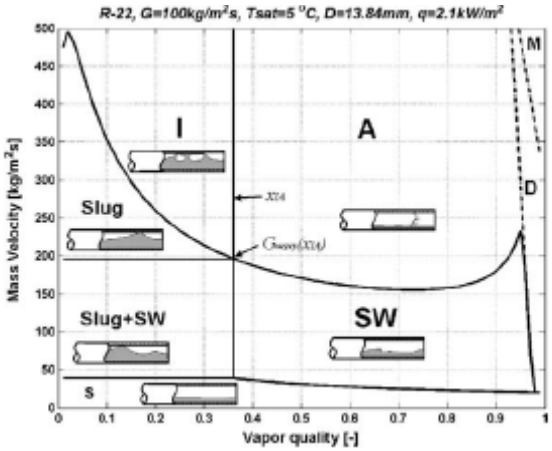


Figure 1. Typical Steiner type flow map taken from Wojtan et al. (2005)

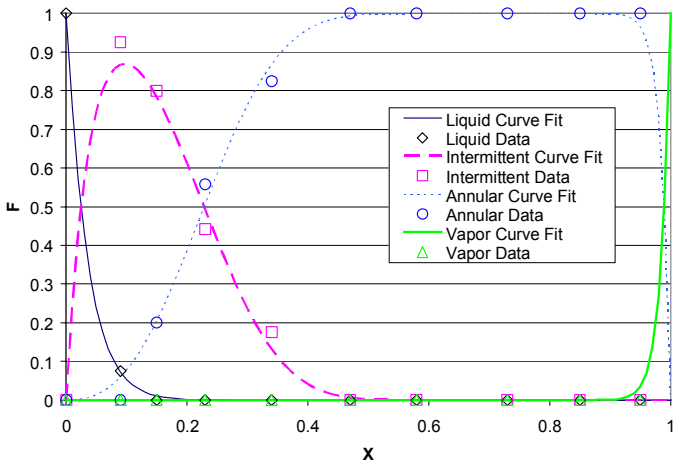


Figure 2. Probabilistic flow map with time fraction curve fits for R410A, 10° C, 300kg/m$^2$-s in a 6-port 1.54 mm hydraulic dia. microchannel taken from Jassim and Newell (2006).

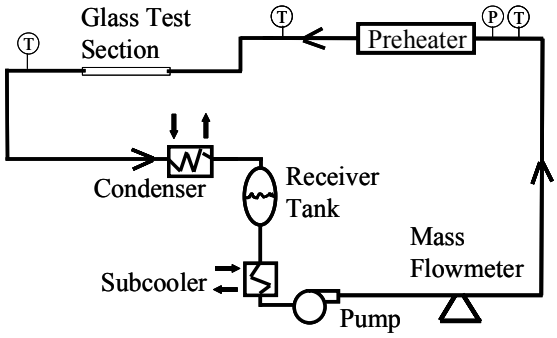


Figure 3. Two-phase flow loop schematic

$$\left(\frac{dP}{dz}\right)_{total} = F_{liq}\left(\frac{dP}{dz}\right)_{liq} + F_{\text{int}}\left(\frac{dP}{dz}\right)_{\text{int}} + F_{vap}\left(\frac{dP}{dz}\right)_{vap} + F_{ann}\left(\frac{dP}{dz}\right)_{ann} \quad (1)$$

$$\alpha_{total} = F_{liq}\alpha_{liq} + F_{\text{int}}\alpha_{\text{int}} + F_{vap}\alpha_{vap} + F_{ann}\alpha_{ann} \quad (2)$$

In this way pressure drop and void fraction models developed for a particular flow regime are easily and properly weighted for the entire quality range on a consistent basis.

The difficulty with this probabilistic flow map based modeling technique is that large numbers of pictures must be classified for each flow condition in order to create a large number of flow maps necessary to generalize the time fraction functions with respect to refrigerant properties and flow conditions. Plazk and Shedd (2003) developed an automated image recognition software to automatically detect the flow regime present from a series of images at a given flow condition. Consequently, this software is suitable for the formulation of traditional Steiner, Baker/Mandhane, and Taitel-Dukler type flow maps. The present study develops image recognition software that determines the flow regime present in each image for a series of images at each flow condition in order to formulate the time fraction of each flow regime to create probabilistic flow regime maps.

In the present study probabilistic two-phase flow maps are experimentally developed for 1.74 mm, 3.9mm, 5.4mm, and 8mm diameter adiabatic tubes for R134a at 25, 35 and 50° C and R410A at 25 ° C saturation temperatures and for a range of mass fluxes and qualities in order to aid in the future modeling of two-phase pressure drop, void fraction, and heat transfer. A diffuse white film pigmented with evenly spaced black stripes are placed in the

background of the tube in the flow visualization experiments to enhance the images and aid in the image recognition process. Nearly 1 million flow visualization pictures were utilized in the formulation of the probabilistic two-phase flow regime maps.

## 2. MATERIALS AND METHODS

### 2.1 Two-phase flow loop and test section design

Flow visualization data was obtained from the two-phase flow loop depicted in figure 3. The liquid refrigerant is pumped with a gear pump that is driven by a variable frequency drive from the bottom of a 2 liter receiver tank through a water cooled shell and tube style subcooler in order to avoid pump cavitation. The liquid refrigerant then travels through a corriolis style mass flow meter followed by a preheater used to reach the desired quality. The preheater consists of a finned tube heat exchanger with opposing electric resistance heater plates bolted on either side of the heat exchanger. The electric heaters are controlled with on/off switches and a variac to provide fine adjustment of quality. This preheater design has enough thermal mass so that the heaters do not burn out at a quality of 100% and has a small enough thermal mass so that steady state conditions can be rapidly attained. The refrigerant is then directed through 90 degree bends to remove effects of heat flux from the preheater such as dryout before it reaches the test section.

The test sections consists of glass tube with dimensions as listed in table 1. The 8mm I.D. test section is 0.254m long since the inner diameter of the incoming copper pipe was also 8mm. The 5.4 mm and 3.9mm test sections are 1.2m long and were transitioned into gradually in order to avoid transition effects. The 1.7 mm I.D. tube is 0.254m long to avoid fracture and excessive pressure drop and was gradually reduced into from the 8mm ID tube to avoid entrance effects. Brass compression fittings with nylon ferrules were used to join the copper pipe of the flow loop to the glass test section in order to avoid leakage or fracture of the test section. The refrigerant is condensed after the test section in a flat plate heat exchanger with cold water at 5$^{o}$ C. The loop temperature is controlled by varying the flow rate of the cold water entering the condenser.

Table 1. Test section and stripe dimensions

| test section I.D. | test section O.D. | test section length | stripe width | center to center stripe distance | distance of striped film fom centerline of tube |
|---|---|---|---|---|---|
| 8.00 mm | 12.70 mm | 0.254 m | 2.1 mm | 5.1 mm | 48 mm |
| 5.43 mm | 9.53 mm | 1.2 m | 1.1 mm | 3.5 mm | 36 mm |
| 3.90 mm | 6.35 mm | 1.2 m | 0.8 mm | 2.1 mm | 20 mm |
| 1.74 mm | 3.00 mm | 0.254 m | 0.3 mm | 1.0 mm | 3 mm |

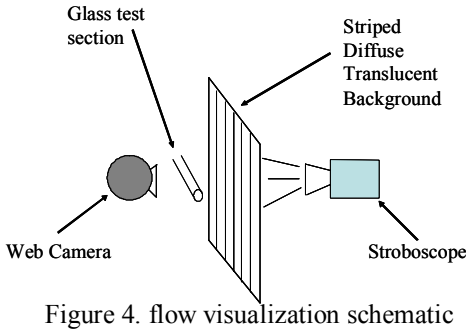


Figure 4. flow visualization schematic

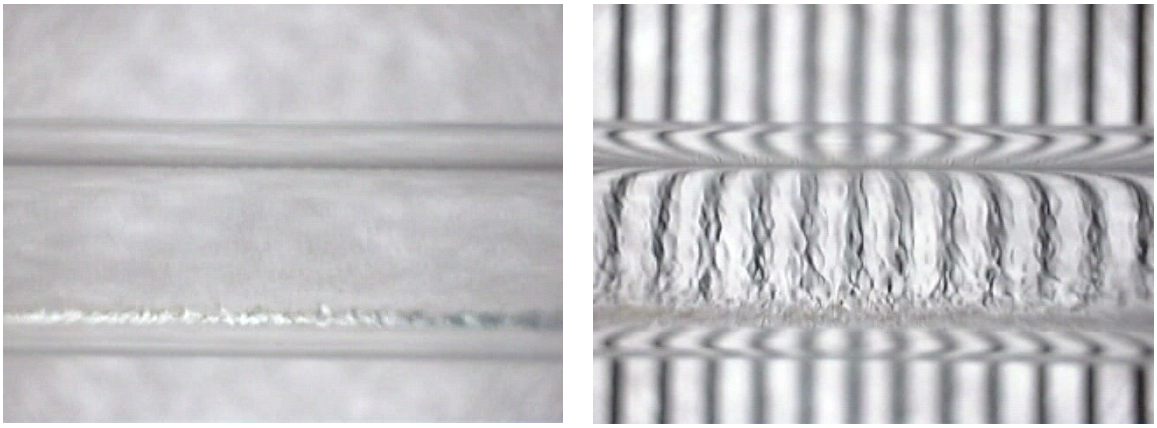

Figure 5 flow visualization pictures of R410A, 3.9mm I.D. tube, 200kg/m^2-s, 0.99 quality, and 25 degrees C with a plane diffuse background (left) and with a striped diffuse background (right)

### 2.2 Flow visualization technique

A unique web camera based flow visualization technique was developed and used in this study as depicted in the schematic in figure 4. A CCD type web camera taking 640x480 pixel pictures at 30 frames per second is used to capture the images. A diffuse white film pigmented with evenly spaced black stripes are placed in the background (behind the glass tube) and illuminated with a stroboscope directed towards the camera. The stroboscope is also cycled at 30 frames per second in order to create clear images. The stripe width, spacing, and distance from the centerline of the test sections are indicated in table 1. These dimensions were determined to best enhance the detection of fine films, and are varied according to pipe diameter to maintain approximately the same stripes per pipe diameter and the same stripe width and spacing per pipe diameter.

The striped background serves to enhance the image as seen in figure 5. Both images in figure 5 were taken for R410A in 3.9mm I.D. tube, a mass flux of 200kg/m$^2$-s, a 0.99 quality, and at a 25$^o$ C saturation temperature with the same diffuse background material. However, the image on right has evenly spaced black stripes on the background. The black stripes provide contrast that enhances the image and allows for the detection of fine films. Furthermore, these stripes aid in the image recognition process. The stripes appear to be out of focus in figure 5 because the camera focal length is adjusted to the center of the tube and not the stripes in the background.

### 2.3 Flow visualization test matrix

Flow visualization pictures were taken for the following test matrix:

- R134a at 25$^o$ C, 35$^o$ C, and 49.7$^o$ C and R410A at 25$^o$ C
- 8mm, 5.4mm, 3.9mm, and 1.74mm I.D. glass test sections
- mass fluxes of 400, 500, 600 kg/m$^2$-s for the 1.74mm ID test sections
- mass fluxes of 100, 200, 300, 400 kg/m$^2$-s for all other tube sizes
- qualities from 0 to 100%

Approximately 30 seconds of flow visualization video (900 images) were taken for each flow condition.

### 2.4 Image recognition software development

Image recognition software was developed in order to automatically classify the flow regime of the obtained images. The original image is first converted into a black and white image as seen in figures 6a, 7a, 8a, and 9a for different conditions. Next, the pixels are thresholded to a percentage of the brightness of the white background as seen in figures 6b, 7b, 8b, and 9b. This percentage varied based upon tube type since the light intensity changed as the distance of the background from the centerline of the tube varied with tube size. It should be noted that thin vertical black lines are drawn between the vertical stripes in figures 6b, 7b, 8b, and 9b for illustration purposes and will be discussed later. If the threshold value is set correctly, the vapor to liquid interface will appear black. The black stripes which normally appear through the tube from the background during liquid flow as seen in figure 6b are bent/scattered horizontally when vapor is present in the tube as seen in figures 7b, 8b, and 9b for intermittent stratified and annular flows respectively. Consequently, black regions are found in the normally white space of the thresholded images. This phenomena is utilized in the image recognition process to detect the presence of vapor at a given tube location. The vertical pixel lines that lie directly between the black stripes seen through the tube when all liquid is present are always white with the maximum pixel value of 256 as seen in figure 6b. Vertical black lines were drawn in the thresholded images in 6b, 7b, 8b, and 9b to indicate the location of the pixel lines that were scanned. If all of the pixel values in all of the vertical pixel lines scanned are above 255, i.e. unbroken as in figure 6b, then the flow is classified in the liquid flow regime. If the flow has one or more broken lines and one or more of the lines is unbroken vapor and liquid regions are detected respectively and hence the flow is classified as intermittent flow. If all of the scanned lines are broken a motion sensor algorithm is used whereby each pixel value in the previous frame is subtracted from the pixel value in the present frame. The image is then thresholded again to remove the noise in the picture as depicted in figures 8c and 9c. The threshold pixel value is determined by observing the minimum value by which no motion is detected when the tube is filled with stagnant vapor. If no white pixels are detected at the top of the tube in a 30 pixel high region, indicated between the horizontal white lines drawn in figure 8c, the image is classified as stratified flow. If one or more white pixels, indicating motion, are detected at the top of the tube in the same region as seen in figure 9c the image is classified as annular flow. In this way the software loops through each image and classifies the flow regime present and keeps a running total of the number of images in each flow regime. The information of the first image is discarded since the motion sensor does not have previous image's pixels to be subtracted. Furthermore, a batch file system was utilized that sequentially reads filenames from a text file and outputs time fraction information to another text file.

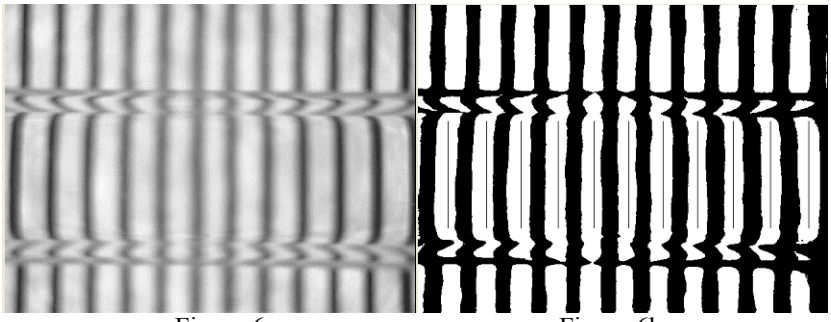

Figure 6a Figure 6b

Figure 6a and b R410A liquid in 3.9mm I.D. glass tube without and with thresholding respectively

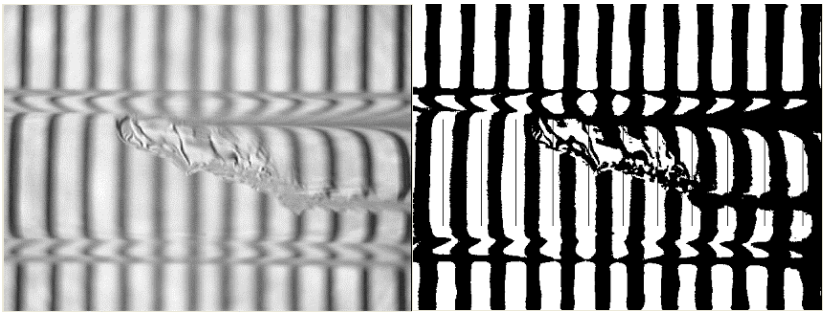

Figure 7a Figure 7b

Figure 7a and b R410A, 0.01 quality, 200kg/m$^2$-s, at 25$^o$ C in 3.9mm I.D. glass tube without and with thresholding respectively

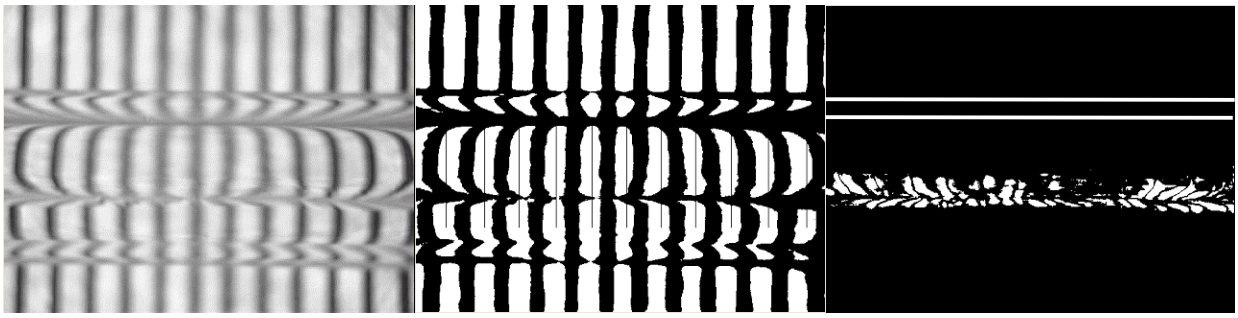

Figure 8a Figure 8b Figure 8c

Figure 8a, b, and c R410A, 0.278 quality, 100kg/m$^2$-s, at 25$^o$ C in 3.9mm I.D. glass tube without thresholding, with thresholding, and thresholded motion sensor respectively

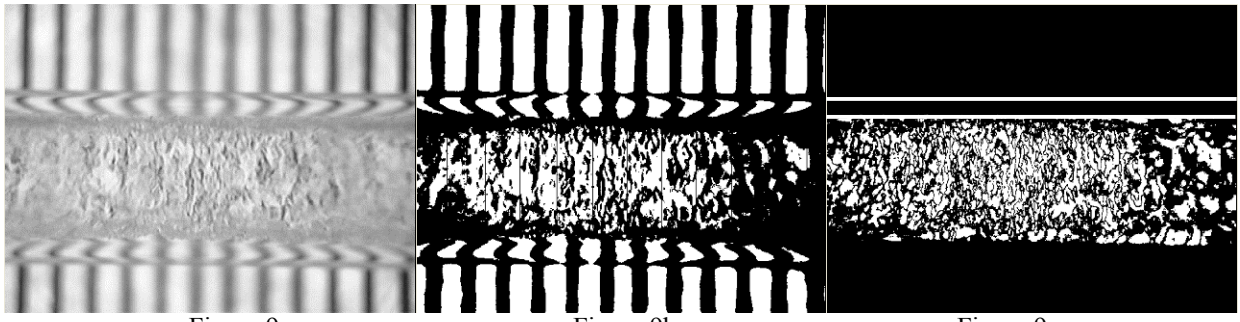

Figure 9a Figure 9b Figure 9c

Figure 9a, b, and c R410A, 0.55 quality, 300kg/m$^2$-s, at 25$^o$ C in 3.9mm I.D. glass tube without thresholding, with thresholding, and thresholded motion sensor respectively

The accuracy of the image recognition software was determined by manually classifying 4800 images of different tube size, mass fluxes, fluids, and qualities. The software is found to have a maximum time fraction error of $\pm$0.04 and an average error of $\pm$0.006.

An alternate algorithm for automated image detection was also used with similar results. In this method the image is thresholded at a lower value than for the first method so that the black stripes from the background appear to be thin but solid. In this case the presence of a liquid vapor interface will bend/scatter the light so that white pixels will appear, i.e. the black stripe is broken, where the solid black stripe exists during liquid only flow. After the image is thresholded the pixel lines located inside the black stripes which appear on the tube from the background during liquid flow are scanned. If all of the pixels in a line are black, pixel intensity of 0, it would indicate that the flow is liquid at that location. If some of the pixels are white, i.e. the black stripe is broken with a pixel intensity of 256, it would indicate that a vapor-liquid interface exists at that location. Consequently, if all of the pixels in the scanned vertical pixel lines are black, the black stripe is unbroken with a value of 0, the image would be classified as liquid flow. If it is not classified as liquid flow (at least one of the scanned pixel lines contains white pixels) and at least one of the pixel lines contains only black pixels, indicating liquid bridging, then the image is classified as intermittent flow. If all of scanned lines contain white pixels then the same motion sensor algorithm is utilized as described in the first method to determine whether the image contains stratified or annular flow.

## 3. RESULTS

Probabilistic two phase flow regime maps were created from the time fraction data collected for the test matrix described above. Figure 10 depicts a probabilistic two-phase flow regime map for R410A flow in the 5.4mm test section with a mass flux of 200kg/m$^2$-s and at a temperature of 25$^o$ C. The solid points in figure 10 represent the time fraction output from the image recognition code developed. The liquid flow regime was considered to be part of the intermittent flow regime hence they are summed together. The annular flow regime time fraction drops off drastically as quality is decreased below 0.2, however there is a minimum at approximately 0.1 quality and the time fraction is seen to increase at lower qualities. This seems to lack a physical basis since theoretically the annular flow time fraction should disappear as quality approaches zero. Furthermore, the intermittent and liquid flow regime should approach 1 as quality approaches 0 since all the flow should become liquid. Therefore, we postulate that that portions of this low quality annular flow is actually intermittent flow with bubbles longer than the field of view. Further investigation with a high-speed camera would be required to verify this postulate. As an approximation a linear time fraction profile was assumed to travel through the origin from a point just before the minimum in annular flow regime time fraction. The difference in time fraction between the raw data and the approximation was added to the intermittent flow regime. The resulting extrapolated intermittent and liquid, and annular flow regimes are plotted in figure 10. Similar time fraction graphs are presented for mass fluxes of 300 and 400 kg/m$^2$-s in figures 11 and 12 respectively. In figures 10 through 12 the uncertainty in quality is less than $\pm$ 0.02 at x=0.99, $\pm$ .012 at x=.5, and $\pm$.002 at x=.02. The uncertainty in mass flux is less than $\pm$2%.

## 4. CONCLUSION

In summary, probabilistic two-phase flow maps have been found in the literature to be useful in the modeling of two-phase flow in multi-port microchannels. A two-phase flow loop was constructed and a new web camera based image recognition technique was developed in order to obtain the flow visualization images necessary to develop probabilistic two phase flow maps for horizontal, adiabatic, single channel tubes. The flow visualization technique utilizes an illuminated striped diffuse background to enhance the images and aid in the image recognition process. Nearly 1 million flow visualization images were obtained for R134a at 25, 35, and 50$^o$C, R410A at 25$^o$C, mass fluxes from 100 to 600kg/m$^2$-s, qualities from 0 to1 in 8mm, 5.4mm, 3.9mm, 1.7mm I.D. smooth adiabatic tubes in order to provide the flow visualization data necessary to generalize probabilistic flow regime maps. Image recognition software was developed in order to classify the flow regime present in each image and formulate the time fraction of each flow regime for a give flow condition. The error in image recognition software in detecting time fraction was found to be a maximum of $\pm$0.04 and an average of $\pm$0.006. In the future, the developed probabilistic two-phase flow maps will be utilized in modeling pressure drop, void fraction, and heat transfer on a consistent two-phase flow map basis.

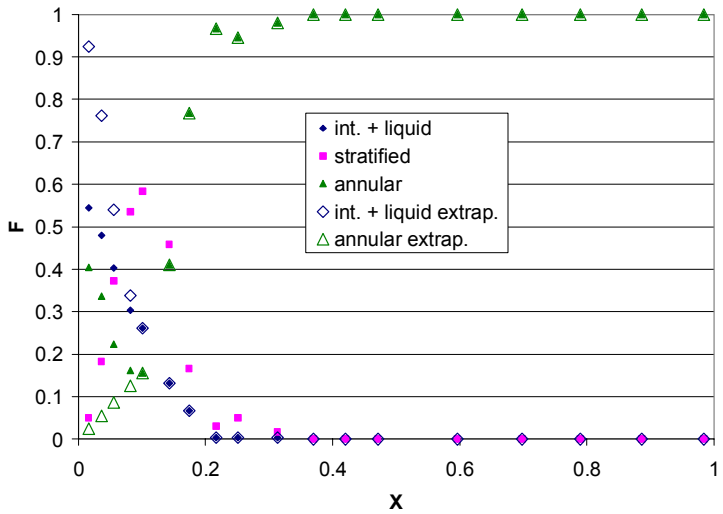


Figure 10. Probabilistic two-phase flow regime map for R410A, 200kg/m$^2$-s, 25$^o$ C, adiabatic 5.4mm I.D. tube

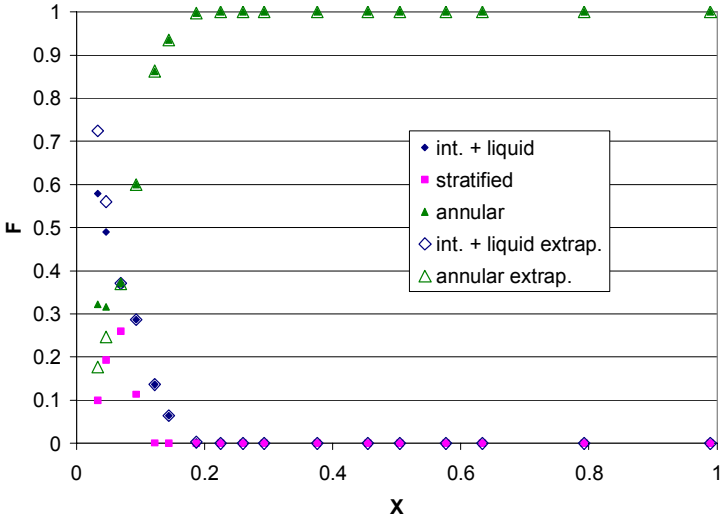


Figure 11. Probabilistic two-phase flow regime map for R410A, 300kg/m$^2$-s, 25$^o$ C, adiabatic 5.4mm I.D. tube

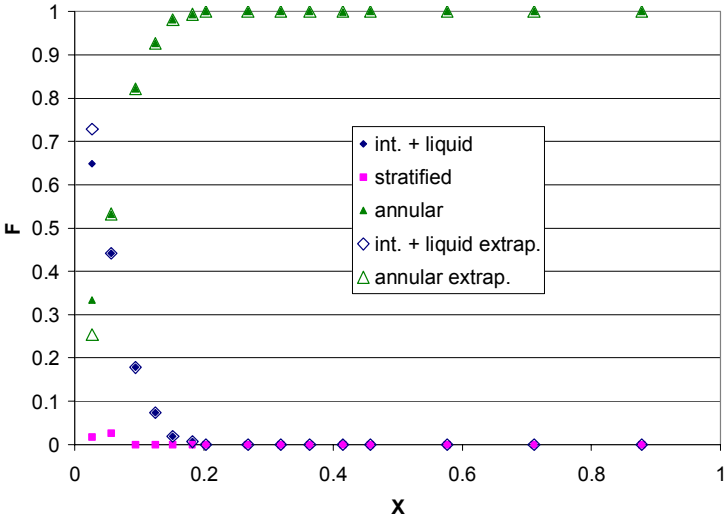


Figure 12. Probabilistic two-phase flow regime map for R410A, 400kg/m$^2$-s, 25$^o$ C, adiabatic 5.4mm I.D. tube

## NOMENCLATURE

| | | | |
|---|---|---|---|
| *dP* | pressure drop (Pa) | **Subscripts** | |
| *dz* | unit length (m) | *liq* | pertaining to the liquid flow regime |
| *F* | observed time fraction (-) | *int* | pertaining to the intermittent flow regime |
| *x* | flow quality (-) | *vap* | pertaining to the vapor flow regime |
| **Greek symbols** | | *ann* | pertaining to the annular flow regime |
| $\alpha$ | void fraction (-) | | |

## REFERENCES


Baker, O., 1954, Simultaneous flow of oil and gas, *Oil and Gas Journal*, vol. 53, p. 185-195.

Coleman, J.W., Garimella, S., 2003, Two-phase flow regimes in round, square and rectangular tubes during condensation of refrigerant R134a, International Journal of Refrigeration, vol. 26: p. 117-128.

Didi, M.B., Kattan, N., Thome, J.R., 2002, Prediction of two-phase pressure gradients of refrigerants in horizontal tubes, International Journal of Refrigeration, vol. 25: p. 935-947.

Dobson, M.K., Chato, J.C., 1998, Condensation in smooth horizontal tubes, Journal of Heat Transfer, vol. 120: p. 245-252.

El Hajal, J., Thome, J.R., Cavallini, A., 2003, Condensation in horizontal tubes, part 1: two-phase flow pattern map, International Journal of Heat and Mass Transfer, vol. 46: p. 3349-3363.

Garimella, S., 2004, Condensation Flow Mechanisms in Microchannels: Basis for Pressure Drop and Heat Transfer Models, Heat Transfer Engineering, vol. 25, no. 3: p. 104-116.

Garimella, S., Killion, J.D., Coleman, J.W., 2003, An Experimentally Validated Model for Two-Phase Pressure Drop in the Intermittent Flow Regime for Noncircular Microchannels, Journal of Fluids Engineering, vol. 125: p. 887-894.

Jassim, E.W., and Newell, T. A., 2006, Prediction of Pressure Drop and Void Fraction In Microchannels Using Probabilistic Flow Mapping. To appear in International Journal of Heat and Mass Transfer.

Mandhane, J.M., Gregory, G.A., Aziz, K., 1974, A flow pattern map for gas-liquid flow in horizontal and inclined pipes, International Journal of Multiphase Flow, vol. 1, p. 537-553.

Niño, V.G., 2002, Characterization of Two-phase Flow in Microchannels, Ph.D. Thesis, University of Illinois, Urbana-Champaign, IL.

Plzak, K. M., and Shedd, T. A., 2003, A Machine Vision-Based Horizontal Two-Phase Flow Regime Detector, *Sixth ASME-JSME Thermal Engineering* Joint *Conference*, Paper 385.

Thome, J.R., El Hajal, J., Cavallini, A., 2003, Condensation in horizontal tubes, part 2: new heat transfer model based on flow regimes, International Journal of Heat and Mass Transfer, vol. 46: p. 3365-3387.

Wojtan, L., Ursenbacher, T. and Thome, J.R., 2005, Investigation of Flow Boiling in Horizontal Tubes: Part I – A New Diabatic Two-Phase Flow Pattern Map, Int. J. Heat Mass Transfer, vol. 48: p. 2955-2969.

Wojtan, L., Ursenbacker, T. and Thome, J.R., 2005, Investigation of Flow Boiling in Horizontal Tubes: Part II – Development of a New Heat Transfer Model for Stratified-Wavy, Dryout and Mist Flow Regimes, Int. J. Heat Mass Transfer, vol. 48: p. 2970-2985.

Zurcher, O., Farvat, D., Thome, J.R., 2002, Development of a diabatic two-phase flow pattern map for horizontal flow boiling, International Journal of Heat and Mass Transfer, vol. 45, p. 291-301.

Zurcher, O., Farvat, D., Thome, J.R., 2002, 2002, Evaporation of refrigerants in a horizontal tube: and improved flow pattern dependent heat transfer model compared to ammonia data, International Journal of Heat and Mass Transfer, vol. 45: p. 303-317.


## ACKNOWLEDGEMENTS

The authors would like to thank the Air Conditioning and Research Center (ACRC) at the University of Illinois for their financial support. The authors would also like to thank Matthew Alonso, Francisco Garcia, Sarah Brewer, Frank Lam for aiding in the data acquisition, and Wen Wu help with Visual Basic.